Available online at www.sciencedirect.com
ScienceDirect
Journal of Catalysis 250 (2007) 190–194
JOURNAL OF CATALYSIS
www.elsevier.com/locate/jcat

Priority Communication

Development of microstructured zeolite films as highly accessible catalytic coatings for microreactors

M.A. Urbiztondo [a], E. Valera [b], T. Trifonov [b], R. Alcubilla [b], S. Irusta [a], M.P. Pina [a], A. Rodríguez [b], J. Santamaría [a,*]

[a] *Nanoscience Institute of Aragon, University of Zaragoza, 50018 Zaragoza, Spain*
[b] *Department of Electronic Engineering, Polytechnic University of Cataluña, Campus Nord. C/. Jordi Girona 1-3, 08034 Barcelona, Spain*

Received 14 May 2007; revised 26 May 2007; accepted 30 May 2007
Available online 5 July 2007

Abstract

Regular structures of SiO_2 microneedles and Si micromonoliths have been formed using processing methods similar to those used in the microelectronics field; then these structures have been used as supports for zeolite (silicalite) films, grown on them by means of seeded hydrothermal synthesis. The procedure leads to microstructured nanoporous coatings with external characteristic dimensions of a few microns in size and short diffusion lengths, allowing intimate fluid–solid contact. Depending on the preparation conditions, the resulting films exhibit values of the external surface to volume ratio in the 400,000–700,000 m^2/m^3 range.
© 2007 Elsevier Inc. All rights reserved.

Keywords: SiO_2 microneedles; Si micromonoliths; Silicalite films; Microreactors

1. Introduction

Nanoporous solids are at the core of various industrial fluid–solid processes, particularly those involving adsorption or catalysis. The challenge of developing an extensive nanoporous structure (in which transport occurs by relatively slow diffusion processes) while at the same time maintaining a high accessibility to the pore network has generally been addressed by reducing the thickness of the porous layer (and thus the length of the diffusion path) and increasing the external solid–fluid contact area. A high external area per unit volume could be obtained by reducing catalyst particle sizes to a few microns, but this would lead to unacceptable pressure drop and severe dust handling problems. To avoid these problems, structured reactors (such as the widely used catalytic monolith converters) have been developed, in which powdered catalysts are replaced by catalytic films deposited as coatings on preformed structures with characteristic lengths (e.g., channel diameter) of several mm.

Reducing channel size even further leads us into the domain of microreactors, where the key feature is the high interfacial specific area (solid/fluid external surface per unit volume) that is available for heat and mass transfer processes (typically in the range of 5000–50,000 m^2/m^3). Thus, impressive benefits have already been demonstrated regarding enhancements in safety, conversion and selectivity that are attainable in microstructured devices for chemical reactions [1,2].

Zeolites seem to be ideal candidate materials for the preparation of catalytic films in microreactors due to their specific properties as catalysts and catalyst supports, as well as the fact that zeolite films can now be grown on a wide variety of surfaces [3]. In addition, the last decade has brought some proposed new applications for zeolite coatings in microchemical systems [4], particularly in microreactors. Some of the methods advocated for the production of miniature zeolite films result from the adaptation of semiconductor fabrication procedures. Thus, Jansen and van Rosmalen [5] were among the first to describe the growth of continuous zeolite films on silicon wafer. Some years ago den Exter et al. [6], reported the preparation of SIL-1 (silicalite) oriented monolayers on silicon wafers that were selectively etched to yield unsupported thin zeolite lay-

* Corresponding author. Fax: +34 976 762142.
E-mail address: jesus.santamaria@unizar.es (J. Santamaría).

0021-9517/$ – see front matter © 2007 Elsevier Inc. All rights reserved.
doi:10.1016/j.jcat.2007.05.022

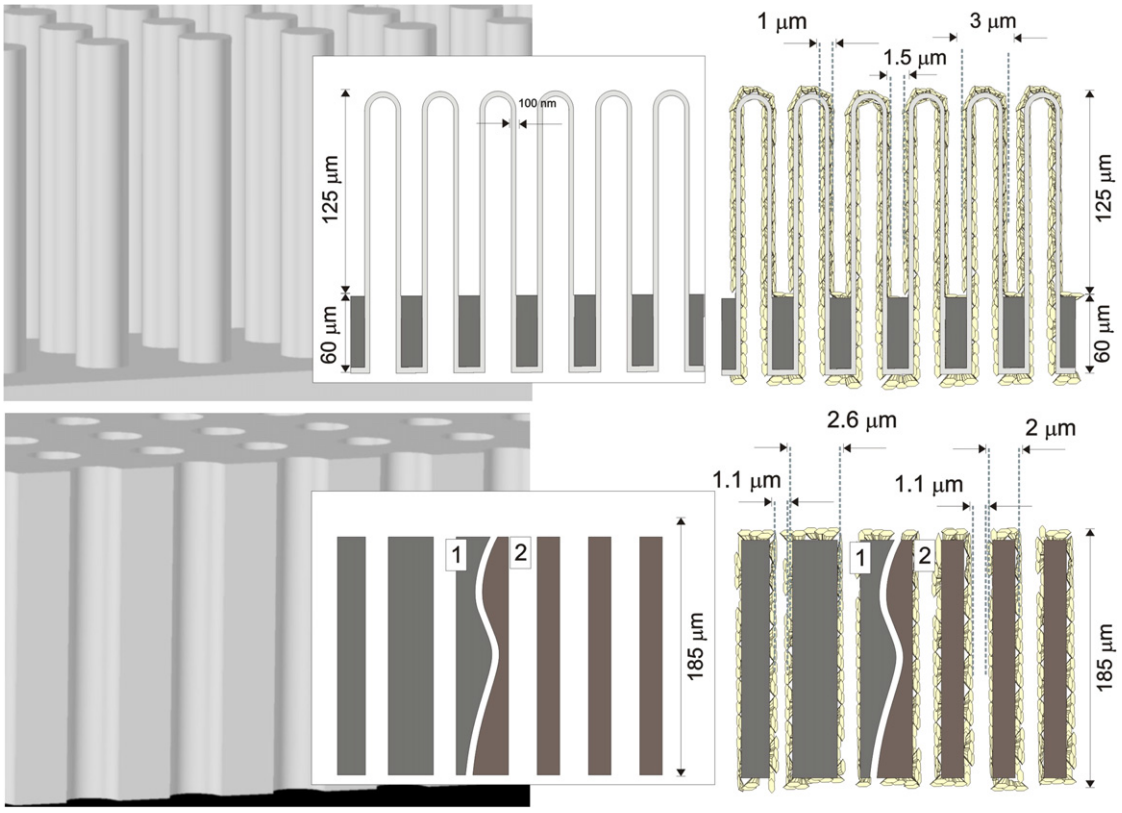

Fig. 1. Scheme and key dimensions of the microneedles (top) and micromonoliths (bottom, where 1 and 2 correspond to structures with a different pore spacing). The left part of the scheme in the drawings shows the starting microstructure, while the right shows the result after coating with zeolites (shown as crystals on the surface of the microstructures). The dark grey areas represent the remaining silicon. 185 microns represent the maximum lenght attainable for microneedles and monoliths on the wafers used. Actual lenghts depend on the preparation method.

ers. In addition, Yeung and coworkers [7,8] have successfully demonstrated how microelectronic technologies can be adapted for the production of miniature membrane reactors and separators.

In this work, nanostructured coatings (SIL-1 films) have been produced on two types of microstructures, micromonoliths and microneedles. Toward this end, photoassisted electrochemical etching was used to create the supporting microstructures (on Si or SiO_2 substrates), and then a seeded synthesis method was used to coat them with a polycrystalline SIL-1 layer. The coating was deposited uniformly and, most importantly, preserves the starting microstructure, allowing the development of robust contactors (reactors, adsorbers) with unprecedented density of external (i.e., fluid–solid interface) area.

2. Experimental

2.1. Formation of the underlying microstructures

Preparation of the supporting microstructures required the formation of straight macropores (2–3 μ in diameter) on ⟨100⟩ *n*-type silicon wafers. The concept (i.e., preexisting microstructure plus added zeolite coating) is shown in Fig. 1 for both micromonoliths and microneedles. The morphology of the macropores, generated by photoassisted electrochemical etching (ECE), depends on anodization conditions, such as current density, etching time, HF concentration, temperature and bias, as well as on substrate properties, such as doping density and orientation [9,10].

Straight macropores were formed on Si wafers by photoassisted ECE in 2.5 wt% aqueous HF electrolyte, because low-concentration hydrofluoric acid leads to pores with high aspect ratios (pore depth/pore diameter). The electrochemical dissolution of silicon proceeds on provision of positive carriers (holes). In *n*-type Si, holes are minority carriers and can be generated by illumination. In this case, a halogen lamp was used, coupled to an IR cutoff filter to prevent hole generation near the surface. The cell for the electrochemical etching comprises a three-electrode system in which the wafer is used as working electrode and two platinum strips are used as counter and reference electrodes. Lithographical patterns were used to define the distance between pores. The front side of the wafer was in contact with the electrolyte, while the backside was exposed to light, with a computer-controlled intensity. The applied voltage was kept constant at 2.4 V by a potentiostat. The basic process flow and etching conditions that ensure stable pore growth have been described previously [9]. Depending on the depth reached with the etching process, SiO_2 microneedles or Si micromonoliths could be produced.

To prepare the microneedles, the process of macropore formation was interrupted before reaching the edge of the wafer, then an underlying structure of SiO_2 was generated by thermal oxidation of the macropore Si walls in dry O_2 at 1100 °C for

Table 1
Synthesis conditions used to obtain SIL-1 coatings on microneedles and micromonoliths

Type of synthesis	Synthesis time and temperature	Gel composition (molar ratio)[a]
Seeded	12 h, 363 K	6TPABr:3TPAOH:25TEOS:4500H_2O
Unseeded	2 h, 398 K	0.32 TPAOH:TEOS:165H_2O

[a] TPABr: tetra-propyl ammonium bromide. TPAOH: tetra-propyl ammonium hydroxide. TEOS: tetra-ethyl orthosilicate.

60–120 min. Next, a backside 25% tetra-methyl ammonium hydroxide (TMAH) etching at 85 °C was performed to release the microneedles. The TMAH etching was stopped just when the pillars reached the desired length (see Fig. 1). To prepare Si micromonoliths the process is similar: once the SiO_2 microneedles have been released, the samples are immersed in BHF solution to dissolve SiO_2, yielding straight, regularly spaced monolith channels. The lenght of these channels can be tailored by controlling the depth of Si removal by TMAH. It should also be noted that a thin SiO_2 layer is readily formed on exposure of freshly etched surfaces of Si to the atmosphere; therefore, the term "Si micromonoliths" as used in this work in fact describes a SiO_2/Si surface.

2.2. Preparation and characterization of zeolite coatings

The silicalite (SIL-1) coatings were obtained by hydrothermal synthesis either on the as-prepared microstructures or after a seeding procedure using aqueous suspensions containing colloidal zeolite [11]. Hydrothermal synthesis [12,13], produced a polycrystalline SIL-1 layer as a coating on the microchannels and microneedles. Table 1 summarizes the synthesis conditions used.

Once the microneedles or micromonoliths had been created, the zeolite coatings were formed using seeded hydrothermal synthesis. Before synthesis, the supports were cleaned in an ultrasonic bath containing acetone and deionized water. Two types of synthesis (seeded and unseeded) were used. The former included a first seeding step aided by treating the microstructured surfaces with mercaptopropyltrimethoxysilane, followed by washing with HCl to get a positively charged surface. The pretreated samples were then immersed in a colloidal SIL-1 suspension (pH 11) prepared according to the recipe of Mintova et al. [11] to anchor the negatively charged SIL-1 seeds onto the supports. After drying at 298 K, the seeding procedure was repeated three times to ensure good coverage of the surface. Then the seeded support was subjected to secondary growth conditions to promote growth of the SIL-1 seeds as described previously [12,13]. For the unseeded synthesis, slight variations in the hydrothermal conditions (concentration, duration, and temperature; see Table 1) were allowed to modify the preferential SIL-1 polycrystalline film orientation and its thickness. After synthesis, the zeolite films were rinsed in distilled water to remove any loosely adherent material. Finally, the composite samples were calcined at 753 K for 8 h (at a heating rate of 0.5 K/min) to remove the organic template.

N_2 physisorption analysis was performed, using a Micromeritics ASAP 2020, to characterize the available specific area for adsorption or catalysis applications. The morphology of the prepared materials were examined by scanning electron microscopy (SEM), operating at 20 kJ (JEOL JSM 6400). X-ray photoelectron analysis (XPS) was performed with an Axis Ultra DLD (Kratos Tech.). The samples were mounted on a sample rod placed in the pretreatment chamber of the spectrometer and then evacuated at room temperature. The spectra were excited by the monochromatized Al$K\alpha$ source (1486.6 eV) run at 15 kV and 10 mA. For the individual peak regions, a pass energy of 20 eV was used. The survey spectrum was measured at a pass energy of 160 eV. The charge-up shift of the XPS peaks were calibrated by taking the Ag $3d_{5/2}$ of silver decoration at 367.9 eV, due to the fact that the C 1s spectrum of the microcapillaries, in addition to the usual adventitious carbon at 284.9 eV, showed the presence of an important contribution at 285.7 eV related to the remaining TMAOH used for Si etching.

XRD analyses were carried out with a Rigaku/Max System using Cu$K\alpha$ radiation ($\lambda = 1.5418$ Å) from 5 to 40° with a step size of 0.03° and a step time of 2.5 s. The data were compared with SIL-1 patterns from the International Zeolite Association Structure Commission.

3. Results and discussion

Examples of the structures formed after zeolite synthesis are shown in the SEM micrographs of Figs. 2 and 3, corresponding to coatings prepared using the seeded synthesis conditions (Table 1) on micromonolith and microneedle supports, respectively. Fig. 2 shows that the growth of the silicalite seeds gave rise to a continuous layer over the surfaces of the Si micromonolith. It is remarkable that the silicalite coating does not appear to plug the pores of the monolith, forming instead a uniform coating on its surface. The zeolite films shown in Fig. 2 have specific external areas of 760,000 (top) and 646,000 (middle) m^2 per m^3 of micromonolith. Despite this high area density, the open space of the micromonolith remains substantial, with >50% of the cross-section in the top monolith and approximately 35% of that in the middle one available for convective flow. The low thickness of the zeolite coatings (ca. 0.5 μm) provides a very short diffusion length, which, coupled to the large interfacial area, makes all of the catalytic material easily accessible.

The bottom micrograph corresponds to a transversal cut of the monolith shown at the top of Fig. 2. It is worth noting that even inside the narrow micromonolith channel, the silicalite seeds have grown into a well-developed zeolite film coating the monolith walls, while leaving the inner channel open. This was made possible by the considerable dilution of the gel used; the concentrated gels readily caused plugging by zeolite lumps at the pore entrance.

Similarly, well-intergrown silicalite layers completely covering the surface of the microneedles were achieved using the same hydrothermal conditions (see Fig. 3). As in the case of the micromonoliths, the bridging of structural spaces by zeolite growth was largely avoided. Instead, despite the tight packing

of the initial microstructure, the needles preserved their individuality after coating by the zeolite film. In this case, applications for fluid–solid contact would involve convective flow of the fluid phase between the microneedles, rather than on their inside. The regularly spaced microneedle network provides excellent accessibility to the zeolite coatings and an external specific area $>460{,}000\ m^2/m^3$ for the structures of Fig. 3.

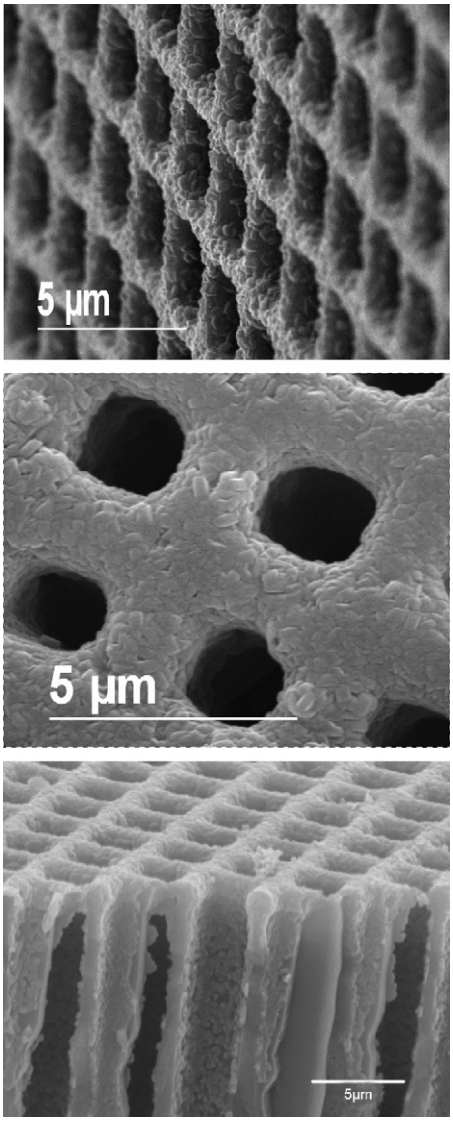

Fig. 2. Different views of zeolite coatings on micromonoliths obtained by seeded synthesis conditions on supports with different grid (macropore) spacings.

Changing the synthesis conditions (especially the gel composition and the shift from seeded to unseeded synthesis) had a dramatic effect on the characteristics of the zeolite coatings obtained. Thus, when the unseeded synthesis conditions listed in Table 1 were used, a preferentially "b"-oriented SIL-1 layer was obtained coating the Si surface between the SiO_2 microneedles, but the microneedles themselves were largely spared from zeolite growth (not shown). In this case, the synthesis conditions and the absence of a seed layer facilitated the partial dissolution of the Si wafer. The increased concentration in this region favored nucleation of new crystals, which grew preferentially along the Si base surface rather than on the microneedles.

In all cases, XRD analysis (not shown) clearly displayed the characteristic SIL-1 diffraction peaks on zeolite-coated microneedles and micromonoliths as the single crystalline phase present; this is in contrast with the results found for as-prepared microneedles and micromonoliths, where only amorphous diffraction patterns were recorded.

XPS analysis on zeolite-coated and uncoated microneedles also confirmed the excellent coverage of the microneedle structure by the zeolite films. The uncoated microneedles showed a Si 2p peak at 102.4 eV that is the result of contributions from the Si substrate (99.6 eV) and the SiO_2 microneedles (103.6 eV) [14]. In contrast, the zeolite-coated material exhibited an Si 2p BE at 103.1 eV. This value is in agreement with values reported for siliceous zeolites [15], indicating that all of the microneedles and the Si substrate are well coated by the silicalite film. Finally, N_2 physisorption analysis on the zeolite-coated microneedles also confirmed the development of a microporous film on the starting microstructures. For the uncoated microneedles, the specific surface was 5.4 m^2/g, with pores located only in the macropore region. In contrast, N_2 adsorption for the composite material revealed a type I isotherm, characteristic of microporous materials. The specific area of 126 m^2/g allows estimation of the proportion of SIL-1 coating at 40% by weight in the zeolite-coated sample.

In summary, the procedure presented in this work (i.e., creation of a regular microstructure followed by seeded hydrother-

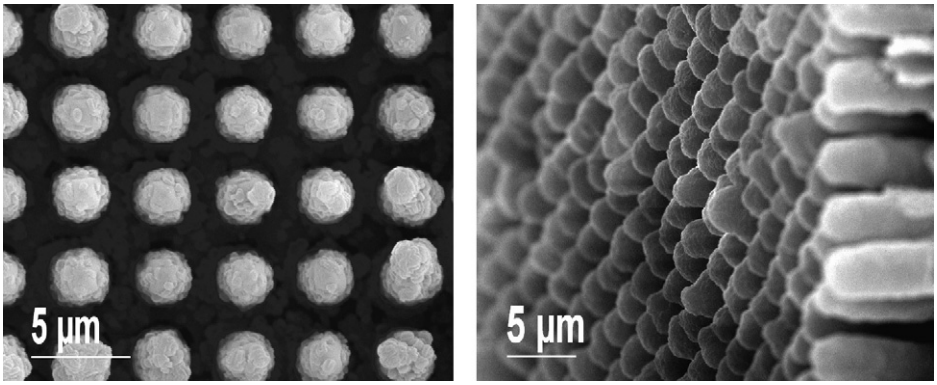

Fig. 3. Top (left) and lateral (right) views of zeolite-coated microneedles. Seeded synthesis conditions.

mal synthesis, producing a nanoporous coating) allows the preparation of microstructured–nanostructured coatings with extremely high values of external interfacial area (upward from 400,000 m^2/m^3). Convective flow can bring molecules from the fluid phase into direct contact with this interface, providing access to the microporous structure of the material. The procedure described herein can be readily extended to the synthesis of other zeolite coatings and, with necessary adaptations, perhaps to other nanoporous coatings as well.

References

[1] G. Kolb, V. Hessel, Chem. Eng. J. 98 (1–2) (2004) 1.
[2] L. Kiwi-Minsker, A. Renken, Catal. Today 110 (2005) 2.
[3] J. Coronas, J. Santamaría, Chem. Eng. Sci. 59 (2004) 4879.
[4] J. Coronas, J. Santamaría, Top. Catal. 29 (2004) 29.
[5] J.C. Jansen, G.M. van Rosmalen, J. Cryst. Growth 128 (1–4) (1993) 1150.
[6] M.J. den Exter, H. van Bekkum, C.J.M. Rijn, F. Kapteijn, J.A. Moulijn, H. Schellevis, C.I.N. Beenakker, Zeolites 19 (1) (1997) 13.
[7] J.L.H. Chau, Y.S.S. Wan, A. Gavriilidis, K.L. Yeung, Chem. Eng. J. 88 (1–3) (2002) 187.
[8] Y.L.A. Leung, K.L. Yeung, Chem. Eng. Sci. 59 (2004) 4809.
[9] A. Rodríguez, D. Molinero, E. Valera, T. Trifonov, L.F. Marsal, J. Pallarés, R. Alcubilla, Sens. Actuators 109 (2005) 135.
[10] V. Lehmann, U. Grüning, Thin Solid Films 297 (1997) 13.
[11] S. Mintova, V. Valtchev, V. Engström, B.J. Schoeman, J. Sterte, Microporous Mater. 11 (1997) 149.
[12] B.J. Schoeman, A. Erden-Senatalar, J. Hedlund, J. Sterte, Zeolites 19 (1) (1997) 21.
[13] Z. Wang, Y. Yan, Microporous Mesoporous Mater. 48 (2001) 229.
[14] D. Wolffram, M. Ratzke, M. Kappa, M.J. Montenegro, M. Döbeli, Th. Lippert, J. Reif, Mater. Sci. Eng. B 109 (2004) 24.
[15] T. Barr, Zeolites 10 (1990) 760.